Buc, J., Ricard, J., & Meunier, J. (1977) *Eur. J. Biochem. 80*, 593-601.
Cardenas, M. L., Rabajille, E., & Niemeyer, H. (1978) *Arch. Biochem. Biophys. 190*, 142-148.
Cardenas, M. L., Rabajille, E., & Niemeyer, H. (1979) *Arch. Biol. Med. Exp. 12*, 571-580.
Cardenas, M. L., Rabajille, E., & Niemeyer, H. (1984a) *Eur. J. Biochem. 145*, 163-171.
Cardenas, M. L., Rabajille, E., & Niemeyer, H. (1984b) *Biochem. J. 222*, 363-370.
Cornish-Bowden, A., & Cardenas, M. L. (1987) *J. Theor. Biol. 124*, 1-23.
Frieden, C. (1970) *J. Biol. Chem. 245*, 5788-5799.
Furman, T. C., & Neet, K. E. (1983) *J. Biol. Chem. 258*, 4930-4936.
Gekko, K., & Timasheff, S. N. (1981a) *Biochemistry 20*, 4667-4676.
Gekko, K., & Timasheff, S. N. (1981b) *Biochemistry 20*, 4677-4684.
Gregoriou, M., Trayer, I. P., & Cornish-Bowden, A. (1981) *Biochemistry 20*, 499-506.
Hardy, L. E., & Kirsch, J. F. (1984) *Biochemistry 23*, 1275-1282.
Holroyde, M. J., Allen, M. B., Storer, A. C., Warsy, A. S., Chesher, J. M. E., Trayer, I. P., Cornish-Bowden, A., & Walker, D. G. (1976) *Biochem. J. 153*, 363-373.
Meglasson, M. D., & Matschinsky, F. M. (1983) *J. Biol. Chem. 258*, 6705-6708.
Neet, K. E., & Ainslie, G. R., Jr. (1980) *Methods Enzymol. 64*, 192-226.
Neet, K. E., Furman, T. C., & Hueston, W. J. (1982) *Arch. Biochem. Biophys. 213*, 14-25.
Neet, K. E., Tippett, P. S., & Keenan, R. P. (1988) in *Dynamics of Solubilized and Immobilized Enzyme Systems* (Chock, B., & Huang, C., Eds.) pp 28-39, Springer-Verlag, Berlin.
Olavarria, J. M., Cardenas, M. L., & Niemeyer, H. (1982) *Arch.Biol. Med. Exp. 15*, 365-369.
Pettersson, G. (1986) *Biochem. J. 233*, 347-350.
Pollard-Knight, D., & Cornish-Bowden, A. (1982) *Mol. Cell. Biochem. 44*, 71-80.
Pollard-Knight, D., Connolly, B. A., Cornish-Bowden, A., & Trayer, I. P. (1985) *Arch. Biochem. Biophys. 237*, 328-334.
Ricard, J., Meunier, J., & Buc, J. (1974) *Eur. J. Biochem. 49*, 195-208.
Shifrin, S., & Parrott, C. L. (1975) *Arch. Biochem. Biophys. 166*, 426-432.
Storer, A. C., & Cornish-Bowden, A. (1976) *Biochem. J. 159*, 7-14.
Storer, A. C., & Cornish-Bowden, A. (1977) *Biochem. J. 165*, 61-69.
Tanford, C. (1968) *Adv. Protein Chem. 23*, 122-282.
Tippett, P. S. (1981) Ph.D. Dissertation, Case Western Reserve University.
Tippett, P. S., & Neet, K. E. (1982a) *J. Biol. Chem. 257*, 12839-12845.
Tippett, P. S., & Neet, K. E. (1982b) *J. Biol. Chem. 257*, 12846-12852.
Tippett, P. S., & Neet, K. E. (1983) *Arch. Biochem. Biophys. 222*, 285-298.
Viola, R. E., Morrison, J. F., & Cleland, W. W. (1980) *Biochemistry 19*, 3131-3137.
Womack, F. C., & Colowick, S. P. (1979) *Proc. Natl. Acad. Sci. U.S.A. 76*, 5080-5084.

Quantitative Footprinting Analysis. Binding to a Single Site†

Robert Rehfuss, Jerry Goodisman,* and James C. Dabrowiak*
Department of Chemistry, Syracuse University, Syracuse, New York 13244-1200
Received June 19, 1989; Revised Manuscript Received August 24, 1989

ABSTRACT: The theory for measuring ligand binding constants from footprinting autoradiographic data associated with a single binding site is derived. If the ligand and DNA cleavage agent compete for a common site, the spot intensities are not proportional to the amount of DNA not blocked by ligand. The analysis of a single site is experimentally illustrated by using results for the anticancer drug actinomycin D interacting with the duplex d(TAGCGCTA)$_2$ as probed with the hydrolytic enzyme DNase I.

Footprinting analysis utilizes DNA sequencing methodology to locate the binding sites of drugs and proteins on DNA molecules of heterogeneous sequence (Galas & Schmitz, 1978; Lane et al., 1983; Scamrov & Beabealashvili, 1983; Van Dyke et al., 1982). In the footprinting experiment, DNA which has come to equilibrium with a ligand is allowed to interact with a probe capable of cutting the DNA at various sites. From the amounts of the different oligonucleotide fragments produced, one can infer where the ligand binds on the DNA, assuming that ligand bound at a DNA site prevents the probe from cleaving at that site. In quantitative footprinting studies, the amounts of fragments produced in the digest are analyzed to extract individual site binding isotherms and determine ligand binding constants as a function of sequence. It has now been demonstrated that one can obtain binding constants for ligands on large DNA polymers as well as small oligomers (Brenowitz et al., 1986; Carey, 1988; Dabrowiak & Goodisman, 1989; Goodisman & Dabrowiak, 1990; Ikeda & Richardson, 1986; Gunderson et al., 1987; Letovsky & Dynan, 1989; Fish et al., 1988; Brenowitz & Senear, 1989).

For an oligomer with only one binding site, the quantitative analysis of footprinting data is quite simple, but not without pitfalls. In the present paper, we show the correct method for extracting the ligand–DNA binding constant from footprinting

† Supported by American Cancer Society Grant NP-681.

0006-2960/90/0429-777$02.50/0

data for a single-site situation and point out how an apparently sound treatment leads to anomalous results. It is sometimes assumed that the measured autoradiographic spot intensities within a ligand binding site are proportional to the fraction of that site unoccupied by ligand but, as was recently pointed out (Dabrowiak & Goodisman, 1989; Ward et al., 1988), this is true only if the amount of DNA to which the cleavage agent can bind is not significantly changed as ligand is added to the system. For example, with the enzyme DNase I or the synthetic compound Fe-MPE, which cleave DNA with little or no sequence specificity, the proportionality holds well (Ward et al., 1988; Dabrowiak et al., 1989a). Since the ratio of ligand-blocked DNA to unblocked DNA is small for large restriction fragments, the effective concentration of the cleavage agent or probe at a site does not significantly increase as ligand is added. However, if the specificity of the cleavage agent is high and is similar to the specificity of the ligand being studied, the proportionality between spot intensity and fraction of site unoccupied may not hold. This occurs for a case recently examined by us, in which the probe was the cationic metalloporphyrin complex MnT4MPyP and the ligand the antiviral agent netropsin, both of which compete for AT-rich sites on DNA (Dabrowiak et al., 1989b).

In this report, we consider a small oligonucleotide duplex possessing a single actinomycin binding site. In this case, in which ligand and probe compete for a very limited amount of DNA, the lack of proportionality between the autoradiographic spot intensity, on one hand, and 1 minus the occupancy of the site by a drug molecule, on the other, has important consequences We show that incorrectly assuming this proportionality can have a significant effect on the binding constants derived from footprinting data. This explains why the binding constants recently reported from analysis of footprinting data for netropsin and distamycin bound to small oligonucleotide duplexes are anomalously low (Fish et al., 1988). We apply a correct analysis to footprinting data for binding of actinomycin D on a small oligomer and derive the binding constant for this drug.

Experimental Procedures

The self-complementary oligonucleotide $d(TAGCGCTA)_2$ was synthesized on a Biosearch 8600 synthesizer and purified by using a Waters Associates HPLC. The molar extinction coefficient of the oligonucleotide was determined by measuring the difference in optical absorbance of a sample at 259 nm before and after exhaustive digestion with snake venom phosphodiesterase (Sigma) in a buffer of 100 mM ammonium acetate (pH 7.5). The molar extinction coefficient of the mixture of mononucleotides was determined by using the expected molar ratios of the mononucleotides present and their individual molar extinction coefficients. The value of ϵ_M found for $d(TAGCGCTA)_2$ was 1.58×10^5 M^{-1} cm^{-1}. Actinomycin D concentrations were measured optically with a value of ϵ_M of 24 400 M^{-1} cm^{-1} at 440 nm.

The oligonucleotide was labeled at its 5′ end using [γ-^{32}P]ATP/polynucleotide kinase and purified via electrophoresis in a 25% polyacrylamide gel containing 6 M urea (Maniatis et al., 1982). The DNase I footprinting reactions were carried out in a total volume of 8 μL, for 10 min at 25 °C, in a buffer consisting of 10 mM Tris (pH 7.5), 8 mM $MgCl_2$, and 2 mM $CaCl_2$. Thirteen different final drug concentrations between 1 and 12 μM, associated with two separate footprinting titrations, were preincubated with the DNA prior to the addition of the enzyme. The final concentration of DNA present in all experiments was 24.3 μM in base pairs (3.04 μM in duplex) while the enzyme concentration was about 0.2 μM. After the reaction was quenched by the addition of urea, the oligonucleotide products were loaded into a 25% polyacrylamide gel and separated via electrophoresis. The resulting autoradiograms were scanned to yield band areas proportional to concentrations. The intensities derived from three of the cleavage products were used in the analysis in the drug concentration range 1–4 μM.

Single-Site Model

Since DNase I must bind to DNA in order to cleave it, the rate at which cleavage occurs at a particular site i is proportional to ν_p, the probability that an enzyme molecule is bound at that site, or the fraction of sites i having an enzyme molecule bound. If the enzyme digest is allowed to proceed only until about 30% of the DNA is cleaved (the "single-hit" regime), the number of oligonucleotide fragments due to cleavage at i is proportional to the initial cleavage rate. The spot intensity or band area on the autoradiogram corresponding to cleavage at site i, I_i, is proportional to the concentration of the corresponding fragment produced, i.e.

$$I_i = k_i \nu_p \tag{1}$$

with k_i a constant. If the ratio of the ligand-blocked DNA to unblocked DNA is small, the quantity ν_p is proportional to p_i, the probability that site i is not blocked to the enzyme, and to the concentration of enzyme at the site, which will be determined by the fraction of sites available to the enzyme. Then, in eq 1, one can put k_i'[DNase I]$_f p_i$ for $k_i \nu_p$ (k_i' a constant), as in previous work (Ward et al., 1988). In the present, single-site, case, we calculate ν_p by considering a competitive binding equilibrium between the ligand and the probe.

Because the binding constant for the ligand will be higher than that for the probe, a ligand molecule binding at a site will generally displace a probe molecule. If enough probe is available to saturate the site in the absence of ligand ($\nu_p \simeq 1$), ν_p in the presence of ligand will indeed be equal to p_i or $1 - \nu_i$, where ν_i is the fraction of binding site occupied by ligand. However, in general, ν_p will be only approximately proportional to $1 - \nu_i$, and, as we show below, small deviations from the proportionality of the amount of cleavage product to $1 - \nu_i$ can be very important and lead to major errors in equilibrium binding constants derived from footprinting data.

We consider a DNA oligomer, with one site which may be occupied either by the ligand or by the probe, i.e., simultaneous occupancy is not possible. Let c be the concentration of oligomer, P_t the total concentration of probe, and D_t the total concentration of ligand. It should be noted that one generally knows D_t, whereas it is the concentration of free ligand which enters the binding constant expressions. Since there is only one site per oligomer, we suppress the site index i, so that I represents the autoradiographic spot intensity (proportional to the concentration of cleavage product produced in the digest) and ν_b represents the fraction of site occupied by ligand. The "footprinting plot" is I as a function of D_t (Ward et al., 1988; Dabrowiak & Goodisman, 1989).

According to eq 1, I will be proportional to ν_p, where ν_b and ν_p are determined by the equilibrium expressions:

$$K = \frac{c\nu_b}{(c - c\nu_b - c\nu_p)(D_t - c\nu_b)} \tag{2}$$

$$K_p = \frac{c\nu_p}{(c - c\nu_b - c\nu_p)(P_t - c\nu_p)} \tag{3}$$

Here, K is the binding constant for ligand to the site and K_p

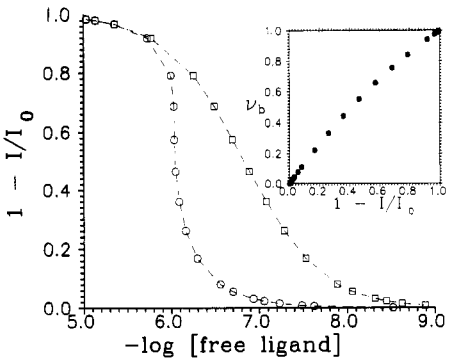

FIGURE 1: Bjerrum plots for a single site using the correct and apparent free ligand concentrations are shown. The inset shows the relationship between the true fraction of site occupied by the ligand, ν_b, and the apparent occupancy as measured from autoradiographic intensities.

the binding constant of the probe to the same site. The object of the analysis of footprinting data is the determination of K: we expect that, for this and similar systems, $K \gg K_p$. In the absence of ligand ($D_t = \nu_b = 0$), ν_p becomes ν_{p0}; eq 3 gives

$$\nu_{p0} = \frac{P_t + c + K_p^{-1} - \sqrt{(P_t + c + K_p^{-1})^2 - 4cP_t}}{2c}$$

Let I_0 be the value of I in the absence of ligand; I_0 is proportional to ν_{p0}.

In the presence of ligand, eqs 2 and 3 must be solved simultaneously. One obtains a cubic equation for ν_p, which may be written

$$[\nu_p^2 c - \nu_p(P_t + c + K_p^{-1}) + P_t][\nu_p c(K - K_p) + K_p P_t] + \nu_p K(\nu_p c - P_t)K_t = 0 \quad (4)$$

Given values for K and K_p, eq 4 may be solved numerically for any desired values of c, P_t, and D_t. Then $I/I_0 = \nu_p/\nu_{p0}$. The data one generally has to analyze consist of experimental values of I, which are proportional to the amount of oligonucleotide produced in the digest, as a function of D_t, with c and P_t constant. Our procedure (Dabrowiak et al., 1989b) is to seek the values of K and K_p which give calculated I as a function of D_t in closest possible agreement with experiment.

The quantity $1 - I/I_0$ is sometimes referred to as the "degree of protection". If one assumes that the degree of protection is equal to ν_b, one can calculate the free ligand concentration as $D_t - c(1 - I/I_0)$ and write eq 2 as

$$K = \frac{1 - I/I_0}{(I/I_0)[D_t - c(1 - I/I_0)]}$$

From a plot of I/I_0 as a function of D_t, one can then easily determine K. As we will now show, such a procedure can lead to large errors because the actual free ligand concentration, $D_t - c\nu_b$, can be very different from $D_t - c(1 - I/I_0)$.

We first show calculated results, based on eq 4, using the experimental parameters $c = 8.85\ \mu M$, $P_t = 1\ \mu M$, and D_t between 0 and 200 μM (Fish et al., 1988). We assume $K = 10^7\ M^{-1}$ and $K_p = 5 \times 10^4\ M^{-1}$. We calculate ν_p, ν_b, and $I/I_0 = \nu_p/\nu_{p0}$ [ν_{p0} is small here (0.0338) because the binding constant K_p is small]. The degree of protection, $f = 1 - I/I_0$, starts at 0 for $D_t = 0$. As D_t increases, f rises, at first almost linearly with D_t, and then levels off as the ratio of D_t to c approaches unity.

In the inset of Figure 1, ν_b is plotted against $1 - I/I_0$. The deviation of this curve from a line of unit slope shows the error in assuming that ν_b is equal to f. Although the deviation does not appear large, it in fact leads to enormous errors in the determination of the ligand binding constant. For an equilibrium like eq 2, one often determines K experimentally by plotting measured values of ν_b against x, the negative logarithm of the free ligand concentration (Bjerrum plot). The value of x for which $\nu_b = {}^1/_2$ should be log K. In Figure 1, f is plotted against x. For the right-hand plot (points represented by squares), which resembles a Bjerrum plot, the correct free ligand concentration is used, i.e., $D_t - \nu_b c$; for the left-hand plot (circles), the apparent free ligand concentration, $D_t - fc$, is used.

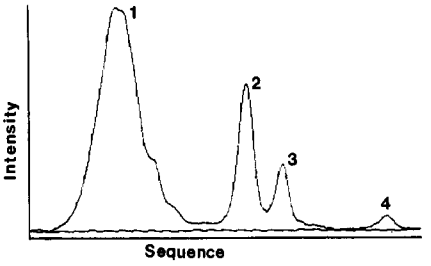

FIGURE 2: Desitometric scan of autoradiographic data of DNase I cleavage of d(TAGCGCTA)$_2$ is shown. The cleavage products represented by peaks 2–4 were used in the analysis. Peak 1 is the uncleaved oligomer.

The two plots are obviously quite different. The left-hand plot does not have a shape like a Bjerrum plot, and the apparent value of K (from the value of x which makes $\nu_b = {}^1/_2$) is close to 10^6, which is an order of magnitude lower than the true value. Even for the values of K_p and K used here, the assumption $f = \nu_b$ leads to very large errors in the free ligand concentration. The correct value of K is obtained from the right-hand plot, $1 - I/I_0$ vs $-\log (D_t - \nu_b c)$. The value obtained for log K is actually slightly below 7 because of the slight difference between $1 - I/I_0$ and ν_b, a difference which has a large effect on the calculated free ligand concentration.

One should expect that, if one plots $f = 1 - I/I_0$ against the negative logarithm of $D_t - fc$, the data may not fit a Bjerrum plot, even if K_p is several orders of magnitude less than K. Indeed, from such a plot, one can judge whether the assumption $f = \nu_b$ is justified. If the shape of the plot is very different from a Bjerrum plot [for example, the slope at $\nu_b = {}^1/_2$ should be $(4 \log e)^{-1}$], a more accurate analysis, such as the following, is required to obtain K.

Actinomycin D Binding to d(TAGCGCTA)$_2$

DNase I cleavage of d(TAGCGCTA)$_2$ produces three major oligonucleotide products, shown in Figure 2. When actinomycin D (Act-D) is added to the system, the amount of each of the products decreases in the manner shown in Figure 3. The fact that no enhancements are observed as drug is added (Figure 3) shows that drug displaces enzyme from the duplex and thus drug and enzyme compete for a common DNA site. For this duplex, with two GC dimers, there are two equivalent binding sites for actinomycin D. However, there is room to bind only one drug molecule to the duplex, so that one bound drug should exclude binding of a second drug or the enzyme. Scott et al. (1988) reported that two actinomycin D molecules can bind to the sequence 5′-GCGC-3′ but that the second drug binds in an anticooperative manner with a binding constant for the second drug a factor of 20 lower than that of the first Act-D molecule. Since only the early part of the footprinting titration was used in this analysis, a duplex possessing two bound Act-D molecules was not part of our model.

We treat the situation as if there were two mutually exclusive binding sites, rather than a single site, and ligand binding at either site blocked cleavage by DNase I. To take into account the presence of two mutually exclusive binding

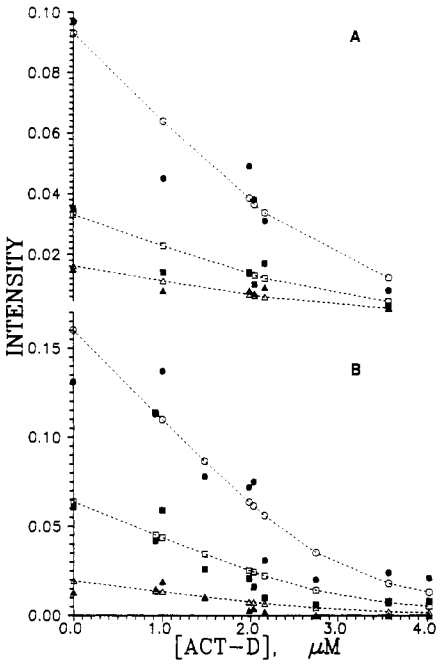

FIGURE 3: Intensities of peaks 2–4 of Figure 2 as a function of actinomycin D concentration. Footprinting plots, for two separate experiments (A and B), are shown. Closed symbols are experimental intensities while the open symbols are the calculated values using the model described in the text.

sites, we have to modify eqs 2 and 3 slightly.

Let K_1 and K_2 be the equilibrium constants for binding of drug at the two sites and ν_1 and ν_2 the fraction of oligomers which have drug bound at the two sites. Then, analogously to eq 2

$$K_1 = \frac{c\nu_1}{(c - c\nu_1 - c\nu_2 - c\nu_p)(D_t - c\nu_1 - c\nu_2)} \quad (5)$$

and similarly for site 2. In eq 3, one has to substitute $\nu_1 + \nu_2$ for ν_b. Adding together eq 5 and the corresponding equation for site 2, we have

$$K_1 + K_2 = \frac{c(\nu_1 + \nu_2)}{(c - c\nu_1 - c\nu_2 - c\nu_p)(D_t - c\nu_1 - c\nu_2)}$$

Thus, we recover eq 2, except that now K represents $K_1 + K_2$ and ν represents $\nu_1 + \nu_2$. The data can be analyzed as a single-site problem, except that, if the two sites are equivalent ($K_1 = K_2$), the resulting equilibrium constant actually represents twice the actual site binding constant.

Two sets of footprinting data, each consisting of autoradiographic spot intensities for three cleaved fragments, were analyzed to obtain the equilibrium binding constant of Act-D. One drug binding site with binding constant K was assumed, such that drug binding blocks the cutting events leading to the three fragments. Thus, the equilibrium binding constant for a single drug binding mode is $K/2$. The analysis involves calculating ν_b as a function of drug concentration, assuming particular values of the binding constants K and K_p, and seeking the values of K and K_p which give the minimum deviation between experimental and calculated data. For each of the two footprinting titrations, the data for all three sites, at all the concentrations shown, were used simultaneously, and fit with the same values of K and K_p.

In Figure 3, we show experimental and theoretical footprinting plots, the latter calculated with the values of K and K_p which minimize D, the deviation between experimental and calculated data. The agreement between experiment and theory is within the experimental error, as judged from the scatter in the experimental points. From the first set of data (Figure 3A), we find $K = 7 \times 10^6$ M^{-1} and $K_p = 10$ M^{-1}; the second set (Figure 3B) yields $K = 9 \times 10^6$ M^{-1} and $K_p = 20$ M^{-1}. In Figure 4, we show, for the data of Figure 3A, D as a function of K_p with K fixed at 7×10^6 M^{-1}, and D as a function of K with K_p fixed at 10 M^{-1}. These plots allow an estimate of the precision of the determined equilibrium constants. The value of K_p, the binding constant of DNase I toward DNA, is not accurately determined. However, it is less than about 10^4 M^{-1}. The determined value of K is good to about $\pm 3 \times 10^6$, since changing K by more than this leads to an increase in D by 10%.

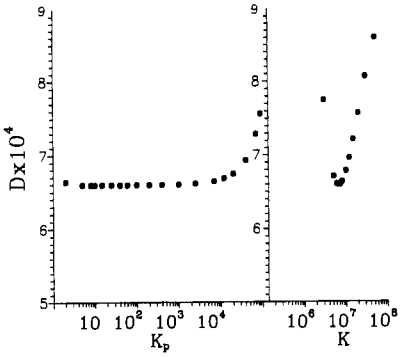

FIGURE 4: Relationship between D, the deviation between experimental and calculated data, and the binding constant of DNase I to DNA, K_p (left panel), and the binding constant of actinomycin D, K (right panel), to DNA.

The Act-D binding constant toward a single site on the 8-mer derived in this study ($\sim 4 \times 10^6$ M^{-1}) is in good agreement with the results of other binding studies using classical techniques. For example, although the salt conditions were not the same as those used in this study, the sequence AGCT in d(ATAAGCTTAT)$_2$ binds Act-D with a binding constant of 5×10^6 M^{-1} (Chen, 1988). The binding constant is somewhat sequence dependent. If the GC site is flanked by C and G, as is the case for d(ATACGCGTAT)$_2$, the binding constant exhibits a slight increase to 8×10^6 M^{-1}. This work confirms the utility of quantitative footprinting analysis for obtaining binding constants of drugs to DNA.

CONCLUSIONS

In this paper, we analyze the footprinting experiment associated with a single site involving a competitive equilibrium between the cleavage agent and a DNA binding ligand. In this case, the lack of proportionality between the autoradiographic spot intensities and 1 minus the occupancy of the site by the ligand has particularly marked consequences. Assuming that the proportionality is valid can lead to measured binding constants which are too low, as seems to have occurred for the recently reported binding constants of netropsin and distamycin, which are significantly lower than those expected for these drugs interacting with the duplex d(GGTATACC)$_2$ (Fish et al., 1988). The analysis presented also applies to protein–DNA footprinting experiments involving DNase I as well as other chemical cleaving agents, e.g., Fe-MPE. If the ratio of protein-blocked sites to free sites on DNA is small, the autoradiographic spot intensities associated with binding will be nearly proportional to the amount of free DNA not blocked by protein. This situation will arise if the fragment on which binding is occurring is long or if it is short but additional nonlabeled DNA is present in the system which can bind the cleavage agent but not the protein. If the fragment is small, the spot intensities will not be proportional to 1 minus the

fraction of site bound by ligand, and care must be taken in the analysis of the data.

Registry No. DNase I, 9003-98-9; d(TAGCGCTA), 115710-85-5; actinomycin D, 50-76-0.

REFERENCES

Brenowitz, M., & Senear, D. F. (1989) *Curr. Protocols Mol. Biol. Suppl. 7* (in press).

Brenowitz, M., Senear, D. F., Shea, M. A., & Ackers, G. K. (1986) *Proc. Natl. Acad. Sci. U.S.A. 83*, 8462-8466.

Carey, J. (1988) *Proc. Natl. Acad. Sci. U.S.A. 85*, 975-979.

Chen, F.-M. (1988) *Biochemistry 27*, 6393-6397.

Dabrowiak, J. C., & Goodisman, J. (1989) *Chemistry and Physics of DNA-Ligand Interactions* (Kallenbach, N. R., Ed.) Adenine Press, Guilderland, NY (in press).

Dabrowiak, J. C., Kissinger, K., & Goodisman, J. (1989a) *Electrophoresis 10*, 404-412.

Dabrowiak, J. C., Ward, B., & Goodisman, J. (1989b) *Biochemistry 28*, 3314-3322.

Fish, E. L., Lane, M. J., & Vournakis, J. N. (1988) *Biochemistry 27*, 6026-6032.

Galas, D. J., & Schmitz, A. (1978) *Nucleic Acids Res. 5*, 3157-3170.

Goodisman, J., & Dabrowiak, J. C. (1990) *Advances in DNA Sequence Specific Agents* (Hurley, L. H., Ed.) JAI Press (in press).

Gunderson, S. I., Chapman, K. A., & Burgess, R. P. (1987) *Biochemistry 26*, 1539-1546.

Ikeda, R. A., & Richardson, C. C. (1986) *Proc. Natl. Acad. Sci. U.S.A. 83*, 3614-3618.

Lane, M., Dabrowiak, J. C., & Vournakis, J. N. (1983) *Proc. Natl. Acad. Sci. U.S.A. 80*, 3260-3264.

Letovsky, J., & Dynan, W. S. (1989) *Nucleic Acids Res. 17*, 2639-2653.

Maniatis, F., Fritsch, E. F., & Sambrook, J. (1982) *Molecular Cloning—A Laboratory Manual*, Cold Spring Harbor, Cold Spring Harbor, NY.

Scamrov, A. V., & Beabealashvili, R. S. (1983) *FEBS Lett. 164*, 97-99.

Scott, E. V., Jones, R. L., Banville, D. L., Zor, G., Marzilli, L. G., & Wilson, W. D. (1988) *Biochemistry 27*, 915-923.

Van Dyke, M. W., Hertzberg, R. P., & Dervan, P. B. (1982) *Proc. Natl. Acad. Sci. U.S.A. 79*, 5470-5474.

Ward, B., Rehfuss, R., Goodisman, J., & Dabrowiak, J. C. (1988) *Biochemistry 27*, 1198-1205.

Thermal Stability of Membrane-Reconstituted Yeast Cytochrome *c* Oxidase†

Paul E. Morin, Diana Diggs, and Ernesto Freire*

Department of Biology and The Biocalorimetry Center, The Johns Hopkins University, Baltimore, Maryland 21218

Received July 10, 1989; Revised Manuscript Received September 7, 1989

ABSTRACT: The thermal dependence of the structural stability of membrane-reconstituted yeast cytochrome *c* oxidase has been studied by using different techniques including high-sensitivity differential scanning calorimetry, differential detergent solubility thermal gel analysis, and enzyme activity measurements. For these studies, the enzyme has been reconstituted into dimyristoylphosphatidylcholine (DMPC) and dielaidoylphosphatidylcholine (DEPC) vesicles using detergent dialysis. The phospholipid moiety affects the stability of the enzyme as judged by the dependence of the denaturation temperature on the lipid composition of the bilayer. The enzyme is more stable when reconstituted with the 18-carbon, unsaturated phospholipid (DEPC) than with the 14-carbon saturated phospholipid (DMPC). In addition, the shapes of the calorimetric transition profiles are different in the two lipid systems, indicating that not all of the subunits are affected equally by the lipid moiety. The overall enthalpy change for the enzyme denaturation is essentially the same for the two lipid reconstitutions (405 kcal/mol of protein for the DMPC and 425 kcal/mol for the DEPC-reconstituted enzyme). In both systems, the van't Hoff to calorimetric enthalpy ratios are less than 0.2, indicating that the unfolding of the enzyme cannot be represented as a two-state process. Differential detergent solubility experiments have allowed us to determine individual subunit thermal denaturation profiles. These experiments indicate that the major contributors to the main transition peak observed calorimetrically are subunits I and II and that the transition temperature of subunit III is the most affected by the phospholipid moiety. Experiments performed at different scanning rates indicate that the thermal denaturation of the enzyme is a kinetically controlled process characterized by activation energies on the order of 40 kcal/mol. These studies have allowed us to quantitatively model the thermal denaturation mechanism of the enzyme.

The formation of functionally active integral membrane protein assemblies involves membrane insertion, folding, and subunit association of the constituent polypeptide units. The molecular details and energetics of those processes are still not completely understood. Cytochrome *c* oxidase is the terminal enzyme of the respiratory chain, catalyzing the transfer of electrons from cytochrome *c* to molecular oxygen while simultaneously serving as a proton pump. Cytochrome *c* oxidase is a multisubunit enzyme composed of mitochondrially synthesized subunits and subunits imported from the cytoplasm. In most species, the three largest subunits (I, II, III) are synthesized in the mitochondria and the remaining subunits

† Supported by grants from the National Institues of Health (GM 37911 and RR 04328).

* To whom correspondence should be addressed.

0006-2960/90/0429-781$02.50/0